A Numerical Study of Methods to Improve Moisture Safety of Ventilated Wooden Roofs

Klaus Viljanen*

Aalto University, Department of Civil Engineering, Rakentajanaukio 4, FI-02150 Espoo, Finland
Ramboll Finland Oy, Itsehallintokuja 3, FI-02600 Espoo, Finland

Laurina Felius

Rambøll Norge AS, Kobbes gate 2, N-7493 Trondheim, Norway

*Corresponding author: **klaus.viljanen@gmail.com**

https://doi.org/10.5755/j01.sace.34.1.35512

Received 2023/11/07

Accepted after revision 2024/01/21

Abstract

The hygrothermal performance of highly insulated, prefabricated wooden roof structures is likely to deteriorate due to the low heat flux to the ventilation cavity. This article evaluates the possibility to improve the moisture safety of such roofs in a Nordic climate by using different control methods for the ventilation rate of the roof and by using thermal insulation above the roof sheathing. The results support the use of adaptive roof ventilation as it decreases the probability of mould growth in the roof. The use of thermal insulation above roof sheathing decreases the probability of mould growth only slightly in a roof with elevated amount of built-in moisture.

Keywords: wooden roof; controlled ventilation; hygrothermal performance; Nordic climate.

Introduction

As a result of increased focus on sustainability, the use of construction wood in Finland has increased. Requirements for the thermal envelope have become stricter in Nordic countries overall, and the reference value of the thermal transmittance (U) of wood-framed roofs in Finland is 0.09 W/(m^{2}K). This requires highly insulated (HI) roof structures, which have an increased moisture risk in the ventilation cavity compared to less insulated structures (Viljanen, 2023).

In the Nordic countries, wood-framed external walls and roofs typically have a ventilated cavity between the wind barrier and the cladding to protect the wind barrier from weather, reducing the risk of leaks, and ensure that the building component can dry out (TenWolde & Carll, 1992; Ingebretsen et al., 2022). As the thermal conditions in the cold season in the ventilation cavity of the roofs are close to the outdoor air (Ojanen & Hyvärinen, 2008; Viljanen, 2023), the moisture conditions in the cavity may deteriorate even with a small moisture load directed to the cavity (Viljanen, 2023; Viljanen et al., 2021; Viljanen et al., 2020).

The hygrothermal performance of roofs may be improved, for example, by designing the roof ventilation (Hagentoft & Sasic Kalagasidis, 2010) and the level of thermal insulation above the cavity (Harderup & Arfvidsson, 2013; Jensen et al., 2020; Viljanen, 2023). Viljanen et al., (2021) identified internal and external R-values, the air change rate of the cavity, and the vapour permeability of the vapour barrier as the most influential parameters for the hygrothermal performance of roofs. The performance of the air cavity improved when the exterior side of the cavity was insulated. To ensure sufficient air flow in the air cavity, the width of the cavity needs to be large enough to reduce pressure losses (Bunkholt et al., 2020). Hydraulic network analysis (HNA) of ventilated roofs shows that with a

ktu 1922

Journal of Sustainable Architecture and Civil Engineering
Vol. 1 / No. 34 / 2024
pp. 101-112
DOI 10.5755/j01.sace.34.1.35512

cavity width of at least 50 mm, the ventilation rate is determined by the pressure losses at the eaves (Viljanen, 2023). The HNA method can be used to design roof ventilation. To avoid snow melt, the ventilation rate of roof cavity should be at least 20 1/h, the ventilation level of which still allows for a small temperature excess in the cavity compared to outdoor air (Viljanen, 2023).

The experimental results of Viljanen (2023) identified the highest risk of mold growth in a ventilated roof with low thermal transmittance at the middle and upper area of the ventilation cavity, whereas in the case of walls, the bottom part of the cavity was most prone to mould growth. To clarify these results, the current study assesses the factors that affect the spatial variation of moisture risks of roofs with low thermal transmittance.

Moisture issues in the ventilation cavities of HI roofs may become more common in the future (Harderup & Arfvidsson, 2013, Nik et al. 2012). The increased moisture content of the outdoor air and precipitation levels in Finland as a result of climate change (Jylhä et al., 2020) will likely further increase the moisture risk (Nik et al., 2012). However, a review study by Ingebretsen et al. (2022) showed that only a limited number of studies have discussed the moisture conditions and microclimate in roof cavities in Nordic countries, most of these originating from Norway.

In this article, the moisture safety of wood-framed, prefabricated roof elements in the current Finnish climate is assessed numerically, and the possibility to improve the moisture safety of these roofs by controlled ventilation or insulation above the roof sheathing is analyzed. The research questions of this study are:

- Is it beneficial to use thermal insulation above the ventilation cavity?
- Is is recommended to have high or low ventilation rate in the cavity or to use adaptive ventilation?
- What is area in the ventilation cavity most prone to moisture issues and why?
- Does the season in which the roof is finished affect the hygrothermal performance of the roof?

The study focuses on low-sloped roofs in present Nordic climate and does not analyse the physical mechanisms behind the level of ventilation in the roof such as buoyancy or forced convection.

Methods

Roof structure, simulation model and model validation

The studied roof structure is a wood-framed, mineral-wool insulated, prefabricated roof element with a U-value of 0.09 W/(m^{2}K). The element includes a 100 mm high ventilation cavity above the insulation, as this is the most common dimension in Finland (Viljanen, 2023). The roof sheathing is a laminated veneer lumber board above which there is a bitumen roofing. Alternatively, there was an additional 20 mm mineral wool board above the roof sheathing. An example of such roof element is presented in **Fig.** 1.

Fig. 1
The installation of wooden roof elements to a building located in Southern Finland

The two-dimensional, time-dependent hygrothermal model was implemented in the commercial software Comsol Multiphysics. The hygrothermal model in this program has been validated as per the standard SFS-EN 15026 (Finnish Standards Association, 2007). However, this validation meth-

od does not include heat and moisture transfer by convection. Thus, the numerical roof model was validated based on the analytical solutions of heat and moisture transfer in the ventilation cavity (Hens, 2007, Nevander & Elmarsson, 2008). The boundary conditions in the numerical model were set steady for the validation phase – outdoor temperature was set to 0°C and outdoor relative humidity to 85 %. The numerical simulation was solved for one year to reach a steady solution for the temperature and humidity distribution in the cavity.

The material layers in the roof structure studied are (from bottom to top): 13 mm thick gypsum board, 0.2 mm polyethylene vapour barrier membrane, 25 mm thick laminated veneer lumber board, 450 mm mineral wool (glass wool), 100 mm thick air cavity, 31 mm thick laminated veneer lumber board (roof sheathing), 20 mm thick rigid mineral wool (glass wool; only in some cases) and a bitumen roofing felt (Fig. 2). The bitumen roofing felt has an s_d-value of about 150 m. The geometry of the roof model is presented in Fig.3. The roof element is 9.6 m long. Because of the high s_d-value, the roofing felt was taken into account in the model by setting the moisture flux on top of the plywood or 20-mm mineral wool to zero and no separate domains were created for the felt. This assumption reduced the length of the simulation time.

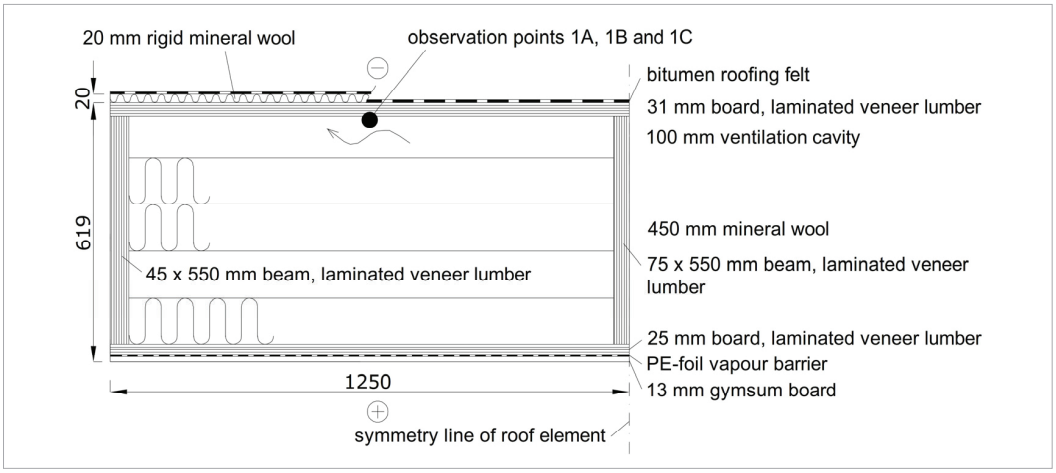

Fig. 2
The studied wood-framed roof element. The symmetry line on the right side of the figure underlines the fact that in reality, a single roof element has two adjacent air cavities

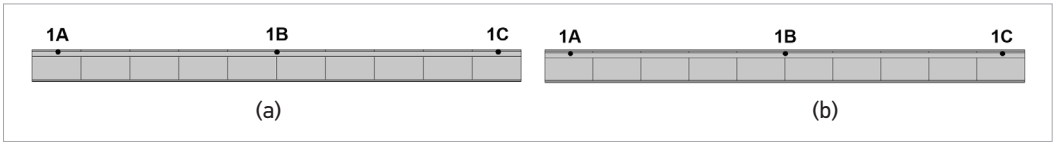

Fig. 3
The geometry of the roof studied used in the numerical model with (a) no insulation above roof sheathing and (b) with 20-mm mineral wool above roof sheathing. The observation points 1A–1C are located at the lower surface of the roof sheathing

Air change in the ventilated cavity

The air velocity in the ventilation cavity was directed from left to right and it was determined according to the following scenarios:

- Cases 1–3 and 5–11: constant air change rate (ACH) in the cavity (5 1/h or 50 1/h)
- Case 4: constant ACH in the cavity (50 1/h) when the outdoor relative humidity is below 75 %. Otherwise, the ACH is 5 1/h.
- Case 12: constant ACH in the cavity (50 1/h) when the absolute humidity in the roof is above the level of the outdoor air. Otherwise, the ACH is 5 1/h.

As the absolute humidity in the roof depends on the amount of ventilation in the roof cavity, the ACH scenario in case 12 induces the most challenge to the numerical solution. To increase the numerical stability of the simulation, the absolute humidity of the roof was monitored not from the outflow air (Fig. 4a) but from the roof materials near the air outflow (Fig. 4b).

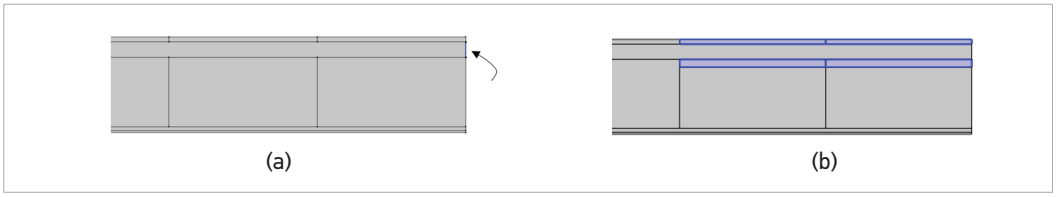

Fig. 4
The monitoring point of absolute humidity in the roof in case 12: (a) a numerically less stable surface area at the outflow to calculate average absolute humidity in cavity air; (b) the purple domains used to calculate the average absolute humidity in the pore air of the materials

Mould growth assessment

The probability of mould growth at the observation points 1A, 1B and 1C (Fig. 3) was evaluated based on the Finnish Mould Growth model (Lähdesmäki et al., 2008; Viitanen et al., 2008). The hygrothermal conditions and material-specific sensitivity classes are included in the model that evaluates the probability of mould growth with a mould index (MI) value. The mould index values vary between 0 and 6, where 0 means no mould growth and 6 means highly abundant mould growth. The parameters used for the roof sheathing board were growth speed 2 (sensitive), maximum amount of mould 2 (sensitive) and decline rate 0.25 (relatively slow). According to the Finnish mould growth model, these parameters apply for wood-based glued boards. Because the parameter values are less sensitive in the case of mineral wool, the mould growth assessment was done only using the parameters for wood-based glued boards and only at the observation points 1A, 1B and 1C. The hygrothermal conditions underside the roof sheathing should favor mould growth as much as the conditions above the mineral wool, and likely even slightly more considering, for example, the cooling of the roof surface by longwave radiation.

Initial humidity, simulation cases and weather conditions

The initial relative humidity in all the materials was 80 %. Thus, the initial amount of moisture represented a normal level of moisture in the roof element. In some cases, the initial relative humidity in the mineral wool or the wood boards was 99 %, which, in the case of mineral wool, corresponds to a moisture content of 10 kg/m^3. Such a level of moisture represents elevated level of built-in moisture or may result from a leaky roofing membrane. The cases with the initial RH of 99 % were used to evaluate the drying-out ability of the roof elements. The simulation cases are described in Table 1.

Table 1
Simulation cases studied; RH denotes relative humidity and AH denotes absolute humidity

Case number	Start of simulation	Initial humidity of materials	Insulation above roof sheathing	Ventilation rate (1/h)
1	1. January	99%-RH for 450 mm mineral wool, other materials 80 %-RH	no	5
2	"	"	no	50
3	"	80 %-RH	no	50
4	"	"	no	50 if $RH_{outdoor}$ <75 %, else 5
5	"	"	20 mm mineral wool	5
6	"	99 %-RH for 450 mm mineral wool, other materials 80 %-RH	20 mm mineral wool	5
7	"	99 %-RH for 450 mm mineral wool, wood boards and 20 mm MW, other materials 80 %-RH	20 mm mineral wool	5
8	"	"	no	5
9	1. October	80 %-RH	no	5
10	"	99 %-RH for 450 mm mineral wool and wood boards, other materials 80 %-RH	no	5
11	"	"	20 mm mineral wool	5
12	"	80 %-RH	no	50 if AH_{roof} > $AH_{outdoor}$, else 5

The weather conditions in the simulation were according to the reference year Vantaa 2017 representing the current weather in Southern Finland. The start of the simulations was scheduled for the cold season and for autumn to evaluate the importance of the season to the hygrothermal performance of the roof. Thus, the first day of the simulation was either January 1st or October 1st. The simulation time was three years, but the mould index values were calculated for the first two years. The moisture production in the indoor space varied between 1–3 g/m^3 depending on the outdoor temperature as per the Finnish guideline (Finnish Association of Civil Engineers, 2022).

Material properties

The heat and moisture transfer related properties of the materials used in the simulation are presented in Table 2 and Table 3.

Table 2
Heat transfer related material properties used in the numerical simulation model

Material	Density (kg/m^3)	Thermal conductivity (W/(mK))	Specific heat capacity (J/(kgK))
Soft mineral wool	23.7	0.037	850
Rigid mineral wool (under roofing)	125	0.031..0.041 (T=-20°C..30°C)	850
Laminated Veneer lumber	510	0.13	1880
Cavity air	1.3	0.025	1005
Gypsum board	660	0.21	870

Table 3
Moisture transfer related material properties used in the numerical simulation model

Material	Water vapour resistance factor (-) 30%-RH, 90%-RH	s_d-value (m)	Hygroscopic moisture (kg/m3) 10%-RH, 98%-RH
Soft mineral wool	1.3		0.3, 6.1
Rigid mineral wool (under roofing felt)	1.3		0.4, 7.2
Laminated veneer lumber	120, 15		15.3, 130
Gypsum board	7, 7		2.6, 25
Polyethylene foil		75	

Radiation heat transfer

The longwave radiation heat transfer between the exterior roof surface and the atmosphere was included in the model when diffuse solar radiation was zero (Fraunhofer Institute for Building Physics 2008). The net emission was calculated by subtracting the atmospheric counterradiation from the estimated radiation heat loss from the roof surface.

The longwave radiation heat transfer between the upper surface of the thermal insulation and the lower surface of the roof sheathing was included in the model based on trial simulations. In the trial simulations, the temperature of the lower surface of the roof sheathing increased 0.5–1.0°C when radiation between these surfaces was included in the model. Longwave radiation at the upper roof surface was not included in the validation phase.

As the hygrothermal conditions propagate in the ventilation cavity, the domains were divided into ten sections in the lateral direction (Fig. 3). Hence, it was possible to calculate the radiation heat transfer in ten sections of the cavity surfaces.

General remarks and model validation

The solution time of the simulation increased substantially if the initial amount of moisture in the insulation was 10 kg/m^3 or if the air velocity in the cavity was not constant. Therefore, the boundary conditions were averaged over 12-hour periods maintaining the time step of

Results

one hour. The averaging was originally made for 6-hour periods, but this resulted in too long simulation times.

The numerical solution of steady state temperature distribution in the roof cavity is close to the analytical solution (Fig. 5). In the numerical solution, the cavity temperature is dominated by convection for the first 0.2 m of the cavity, whereas in the analytical solution, heat conduction increases the air temperature already at distance of 0–0.2 m from the cavity inlet. The difference between analytical and numerical solution is at most 0.2°C. The simulated relative humidity distribution between the distance of 0–4 m from the cavity inlet is slightly above the distribution based on the analytical solution due to the difference in the temperature distribution. The difference in calculated relative humidity is at most 1 %-units between the analytical and numerical solutions.

Fig. 5

Temperature and relative humidity distributions in the cavity according to the different models

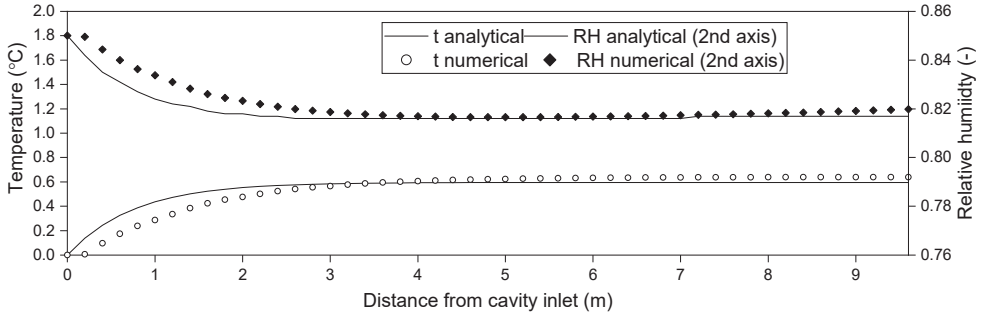

Heat and moisture transfer in the roof

The moisture content of the 450 mm thick mineral wool was low in cases 3, 4, 5, 9 and 12 with low initial level of moisture (Fig. 6a). In cases 1, 2 and 6 the 450 mm thick mineral wool dried faster than in the other cases with an elevated initial level of moisture. The difference in drying rate compared to cases 7 and 8 was relatively small considering that in cases 7 and 8 the relative humidity of all the materials outside the vapour barrier was initially 99 %. The drying of the mineral wool was distinctly slowest in cases 10 and 11, in which case, the mineral wool reached a hygroscopic moisture level (below 1 kg/m^3) only after eight months of simulation.

In cases 2–5, the relative humidity of the roof sheathing rose to at most 85 % and after two months, relative humidity decreased for the next four months reaching a level of 50–55 % (Fig. 6b). In cases 1 and 6, the roof sheathing dried only after three months from the beginning of the simulation. In case 9, the drying of the sheathing began only after five months of the simulation. In cases 10 and 11, the relative humidity of the roof sheathing was above 90 % over seven months and decreased to below 90 % in May. In case 12, the relative humidity of the sheathing was continuously below that solved in case 9. The relative humidity and moisture content results show that the built-in moisture dried out from the simulated roofs in less than one year (Fig. 6).

The difference in temperature between the lower surface of the roof sheathing (points 1A, 1B and 1C) and the outdoor air in cases 1–8 is presented in Fig. 7a, 7c and 7e. In January, the temperature excess was at most 1°C in most of the simulated cases. In cases 5–7 the temperature excess was 1–1.2°C at Point 1A and 2.5–3.4°C at points 1B and 1C. In summer, the temperature excesses at Point 1A were about 6°C in cases 1 and 8 and 3.5–4.2°C in the other cases. At the other observation points the temperature excesses were 6–9 °C in the simulated cases.

In January, the relative humidity at Point 1A on the surface of the roof sheathing was 2–9 %-units below the relative humidity of the outdoor air (Fig. 7b). At the other observation points,

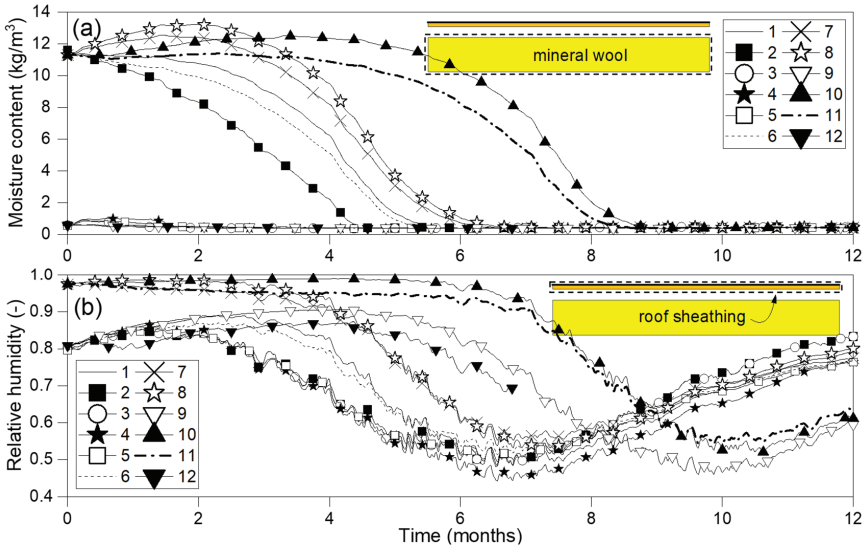

Fig. 6

(a) Moisture content of the thermal insulation; (b) average relative humidity in the roof sheathing; 24-hour avg. values

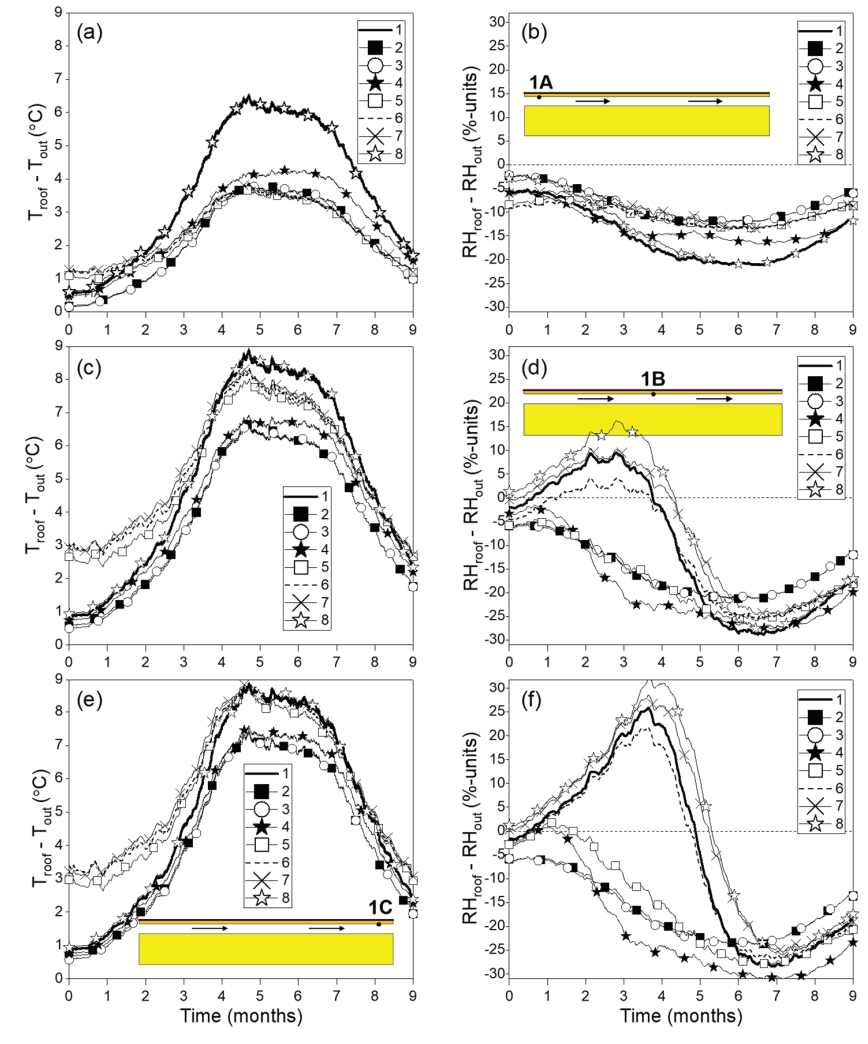

Fig. 7

(a), (c) and (e) Temperature difference between Point 1A/1B/1C and outdoor air; (b), (d) and (f) relative humidity difference between Point 1A/1B/1C and outdoor air (simulation cases 1–8); 42-days avg. temperature difference and 50-days avg. relative humidity difference

the relative humidity increased in cases 1 and 6–8 to above the relative humidity of the outdoor air (**Fig. 7d** and **7f**). At Point 1B, the relative humidity decreased to a level below that in the outdoor air in 4–4.5 months, whereas at Point 1C this took 5–5.5 months. In the beginning of the simulation, the relative humidity at Point 1C was above the outdoor relative humidity for a few weeks in cases 4 and 5.

In cases 9–12, the temperature excess at Point 1A in October was 0.8–1.4°C, whereas at points 1B and 1C the temperature excess was 1.4–3°C (**Fig. 8a**, **8c** and **8e**). In December, the temperature excess at all points was at most 0.5°C. In summer, the temperature excesses were 3.5–6°C (Point 1A) and 7.5–9°C (points 1B and 1C).

In October, the relative humidity at Point 1A in cases 9–12 was 5-8 %-units below the relative humidity of the outdoor air (**Fig. 8b**). At the other observation points, the relative humidity difference between outdoor air was rather constant, but depending on the case, the relative humidity in the cavity was either below or above the level of the outdoor air. The relative humidity at points 1B and 1C was especially low in case 12. In summer, the relative humidity rose distinctly high at Point 1C in cases 10 and 11.

Fig. 8

(a), (c) and (e) Temperature difference between Point 1A/1B/1C and outdoor air; (b), (d) and (f) relative humidity difference between Point 1A/1B/1C and outdoor air (simulation cases 9–12); 42-days avg. temperature difference and 50-days avg. relative humidity difference

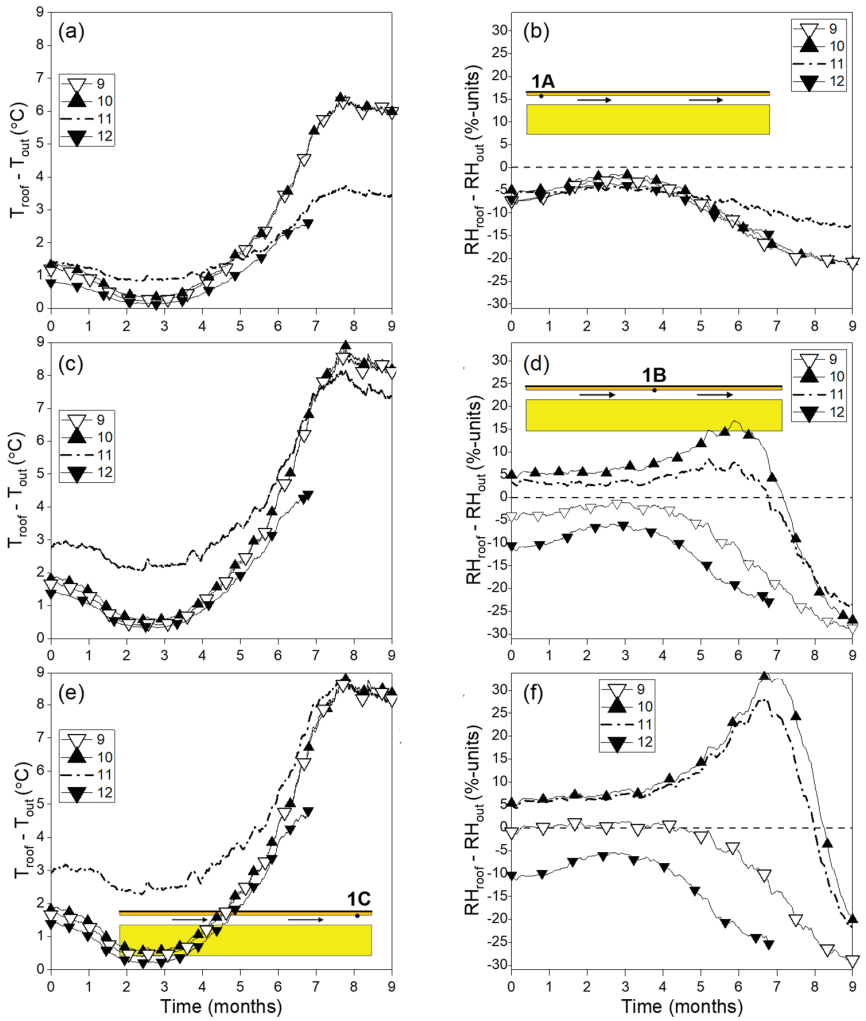

The moisture transfer in the roof was analysed in more detail in the simulation case 10. After 4.7 months of simulation the relative humidity in the inner parts of the roof had decreased to a level of 50 % whereas in the outer parts of the roof the relative humidity was still at the level of 100 % (Fig. 9a). After 7.6 months of simulation the relative humidity in the roof materials near the air inflow was at a level of 30–40 % (Fig. 9b). After 8.5 months the dry area in the roof covered more than half of the roof (Fig. 9c). After 10 months the relative humidity in the whole roof was 40–65 % and the impact of the inflow air, that had higher relative humidity than in the roof, was visible (Fig. 9d). The 2-dimensional RH distributions at the time intervals were consistent with the results in Fig. 8b, 8d and 8f.

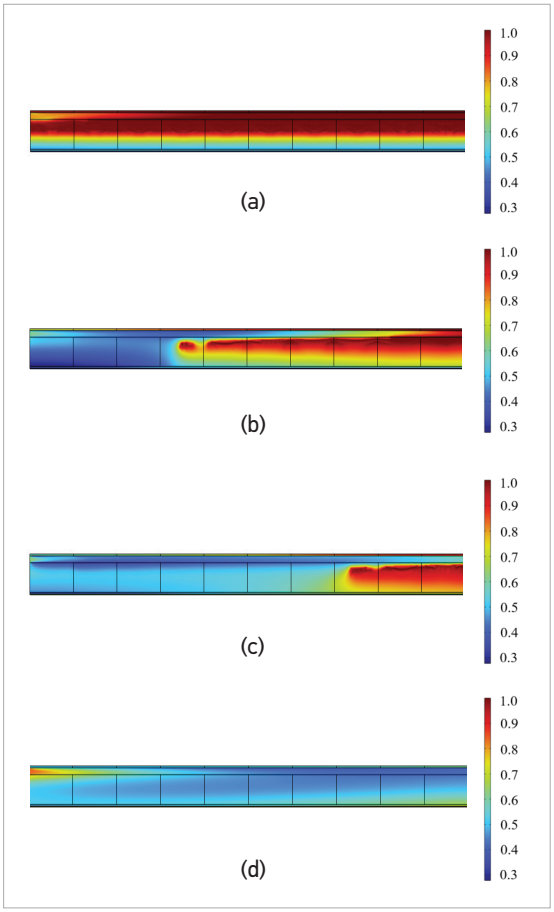

Fig. 9

Relative humidity (-) distribution in case 10 at (a) 4.7 months (141 days), (b) 7.6 months (228 days), (c) 8.5 months (254 days), and (d) 10 months (300 days)

Mould growth assessment in the roof

The maximum values of mould index on the roof sheathing during the three-year simulations are presented in Table 4. In terms of the risk of mould growth, the roofs of simulation cases 2–5, 9 and 12 perform well (mould index 0.01–0.49). In cases 8, 10 and 11, the mould index values at Point 1B are between 1.1 and 2.3. In cases 1, 6–8 and 10–11, the index values at Point 1C are between 1.5 and 4.7. The development of the mould index

Simulation case	Max. mould index at point 1A	Max. mould index at point 1B	Max. mould index at point 1C
1	0.06	0.34	1.57
2	0.47	0.06	0.03
3	0.47	0.06	0.03
4	0.06	0.01	0.03
5	0.11	0.00	0.15
6	0.11	0.08	1.46
7	0.11	0.82	2.66
8	0.06	1.10	2.83
9	0.09	0.17	0.49
10	0.17	2.26	4.71
11	0.16	1.72	4.42
12	0.10	0.03	0.03

Table 4

Mould growth assessment at the bottom surface of the roof sheathing

value at Point 1C is presented in Fig.10. The maximum values of the mould index were reached in the first eight months of the simulation.

Fig. 10
Mould index values at Point 1C during the first two years of the simulation

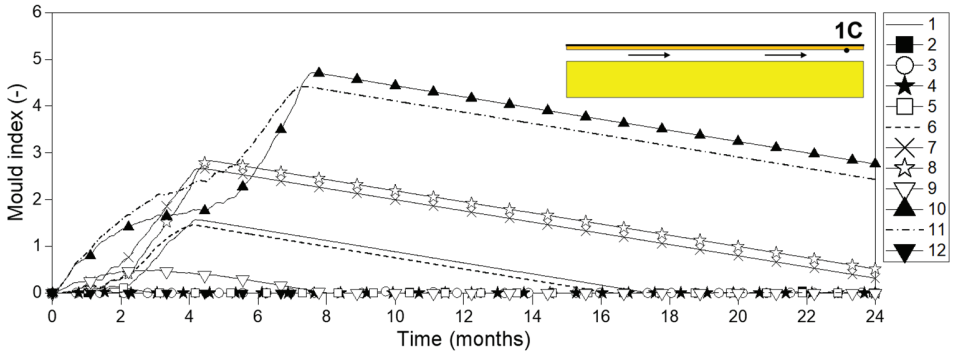

Discussion

The results of cases 1 and 6 imply that the thermal insulation above the roof sheathing increases the drying rate of the mineral wool only slightly. The impact of insulation above the cavity on the mould growth risk at Point 1C is also small (MI 1.46 vs. 1.57), which coinsides with the findings of Nik et al. (2012). The ventilation rate is an important factor that not only increases the drying rate of the roof but decreases the mould growth risk as in case 2 with the ACH rate of 50 1/h the mould index is only 0.03 at point 1C.

The results of cases 1 and 6–8 show that if the level of built-in moisture in a roof is elevated, the highest risk of mould growth is in the direction of the ventilation airflow and near the air outflow. In this area, the drying of the construction is slowest as the airflow dries the area only after the other area in the roof has dried. This was also evident from the 2-dimensional relative humidity distributions at the selected time intervals. These results explain the observed mould risk at the middle and outlet area of a test roof (Viljanen, 2023).

In case 4, the higher ventilation rate only when outdoor relative humidity is below 75 % showed improved performance compared to case 3 with constant ACH of 50 1/h; at Point 1A the mould index decreased from 0.47 to 0.06. A reason for this behaviour is the higher temperatures in the roof cavity in case 4. This result is in accordance with the observation by Viljanen (2023) that the optimal ventilation rate of roofs is about 20 1/h considering both the moisture safety and the risk of snow melt.

The drying rates observed for the mineral wool and the relative humidity of the roof sheathing show the impact of weather conditions to the drying rate. In autumn weather (cases 10 and 11), the drying of humid roof materials is slower than in winter (cases 7 and 8). This resulted in high mould indexes (1.7–4.7) in cases 10 and 11 at points 1B and 1C, whereas in cases 7 and 8, the maximum mould index was 2.8. Nelson (2017) observed lower mould index values (< 2) for walls that started to dry in May compared to January. Therefore, the lowest risk of mould growth in initially humid roofs may occur if the drying starts in the warm season.

In the case of adaptive ventilation rate of the roof cavity (case 12), the simulation experienced difficulties to reach convergence. Thereby the simulation time was shortened to 204 days. The results show that with adaptive roof ventilation the relative humidity of the roof sheathing is lower compared to a constant low air change in the cavity (case 9). Hagentoft & Sasic Kalagasidis (2010) observed similarly that adaptive attic ventilation decreases attic RH compared to natural ventilation. The mould index value at Point 1C decreased from 0.49 to 0.03 by using adaptive ventilation.

Conclusions

This study assessed the factors affecting the moisture safety of wood-framed roof elements in Nordic climate. The results show that a high level of built-in moisture in a wooden roof element or roof leaks lead to a risk of mould growth in the middle area and in the outflow area of the roof. If the roof is finished in autumn, the risk of mould growth arising from increased level of initial moisture is even higher. In some cases, a high level of roof ventilation may prevent this risk. The use of adaptive roof ventilation proved to be a promising approach decreasing the risk of moisture issues in a roof. In practice, such an approach requires to use, for example, fans and measurement sensors. Although the use of a 20-mm thermal insulation above roof sheathing does not prevent mould growth risk in a roof with high amount of built-in moisture, this approach improved the hygric performance of the roof by increasing the drying rate of the thick thermal insulation layer.

Factories manufacturing roof elements should measure and minimize the moisture content of the materials used for the roof elements. Work planning (e.q., weather protection) and quality control in the construction site should ensure that the moisture level of the finished roof is low, which is especially important if the roof is finished in autumn. If the roof elements or the joints between them get wet, the element installations should be stopped to assess the situation by on-site moisture measurements.

The numerical model developed for the study proved to describe the hygrothermal behaviour of a roof reliably. Future studies should analyse the behaviour of the wooden roof elements also in the predicted future weather conditions. In practice, the amount of ventilation in the roof depends on the wind conditions, roof slope and ventilation openings/roof ventilators. Therefore, the temporal variation in the amount of ventilation affects the performance of the roof. A thick layer of snow on the roof in the cold-season may also affect the hygrothermal behavior of the roof, for example, by increasing the temperature in the ventilation cavity and thus, increasing the drying rate of the roof. It is recommended to further assess the effect of these factors in future studies.

Acknowledgment

The authors would like to thank Kari Ovaskainen for providing Fig.1 to be used in the article. The authors gratefully acknowledge and thank Rambøll for financial support.

References

Bunkholt, N.S., Säwén, T., Stockhaus, M., Kvande, T., Gullbrekken, L., Wahlgren, P., & Lohne, J. (2020). Experimental Study of Thermal Buoyancy in the Cavity of Ventilated Roofs. Buildings, 10, 8. https://doi.org/10.3390/buildings10010008

Finnish Association of Civil Engineers (2022). Water and moisture proofing instructions for buildings, RIL 107-2022. Finnish Association of Civil Engineers.

Finnish Standards Association (2007). Hygrothermal performance of building components and building elements. Assessment of moisture transfer by numerical simulation. Standard SFS-EN 15026.

Fraunhofer Institute for Building Physics IBP (2008, September 30). Details:LongWaveExhange. https://www.wufi-wiki.com/mediawiki/index.php/Details:LongWaveExchange

Hagentoft, C. E. & Sasic Kalagasidis, A. (2010). Mold growth control in cold attics through adaptive ventilation: Validation by field measurements. In 11th International conference on thermal performance of the exterior envelopes of whole buildings, Clearwater Beach, FL, USA, 5-9 December 2010. American Society of Heating, Refrigerating and Air-Conditioning Engineers.

Harderup, L.-E. & Arfvidsson, J. (2013). Moisture safety in cold attics with thick thermal insulation. Journal of Architectural Engineering 19(4), 265-278. https://doi.org/10.1061/(ASCE)AE.1943-5568.0000067

Hens, H. (2007). Building Physics - Heat, air and moisture: Fundamentals and engineering methods with examples and exercises. Leuven: Ernst Sohn Verlag.

Ingebretsen, S.B., Andenæs, E., & Kvande, T. (2022). Microclimate of Air Cavities in Ventilated Roof and Façade Systems in Nordic Climates. Buildings, 12, 683. https://doi.org/10.3390/buildings12050683

Jensen, N. F., Bjarløv, S. P., Johnston, C. J., Pold, C. F. H., Hansen, M. H. & Peuhkuri, R. H. (2020). Hygrothermal assessment of north-facing, cold attic

spaces under the eaves with varying structural roof scenarios. Journal of Building Physics 44(1), 3-36. https://doi.org/10.1177/1744259119891753

Jylhä, K., Ruosteenoja, K., Böök, H., Lindfors, A., Pirinen, P., Laapas, M. & Mäkelä, A. (2020). Weather information of the present and future climate for building physical calculations and for the reference year 2020 of energy calculation. Report 2020:6. Finnish Meteorological Institute.

Lähdesmäki, K., Vinha, J., Viitanen, H., Salminen, K., Peuhkuri, R., Ojanen, T., Paajanen, L., Iitti, H. & Strander, T. (2008). Development of an improved model for mould growth: Laboratory and field experiments. In Proceedings of the 8th symposium on building physics in the Nordic Countries (pp.935-942). Danish Society of Engineers.

Nelson, T. B. (2017). Moisture safety in highly insulated wood-frame wall constructions. M.Sc. thesis. Norwegian University of Science and Technology.

Nevander, L. E. & Elmarsson, B. (2008). Moisture handbook. Practice and theory (in Swedish). Solna: Svensk byggtjänst.

Nik, V. M., Sasic Kalagasidis, A. & Kjellström, E. (2012). Assessment of hygrothermal performance and mould growth risk in ventilated attics in respect to possible climate changes in Sweden. Building and Environment 55, 96-109. https://doi.org/10.1016/j.buildenv.2012.01.024

Ojanen, T. & Hyvärinen, J. (2008). Statement on the effects of improving energy efficiency of structures on the hygric behaviour of structures (in Finnish). Research report VTT-S-10816-08, Technical Research Centre of Finland, Finland, December.

TenWolde, A. & Carll, C. (1992). Effect of Cavity Ventilation on Moisture Walls and Roofs. In 5th international conference on thermal performance of the exterior envelopes of whole buildings, Clearwater Beach, FL, USA, 7-10 December 1992, pp. 555-562. American Society of Heating, Refrigerating and Air-Conditioning Engineers.

Viitanen, H., Vinha, J., Peuhkuri, R., Ojanen, T., Lähdesmäki, K. & Salminen, K. (2008). Development of an improved model for mould growth: Modelling. In Proceedings of the 8th symposium on building physics in the Nordic countries (pp.927-934). Danish Society of Engineers.

Viljanen, K. (2023). Hygrothermal performance of wood-framed, mineral-wool-insulated walls and roofs with low thermal transmittance. Dissertation. Aalto University.

Viljanen, K., Lü, X. & Puttonen, J. (2020). Hygrothermal behavior of ventilation cavities in highly insulated envelopes. E3S Web of Conferences 172, 07003. https://doi.org/10.1051/e3sconf/202017207003

Viljanen, K., Lü, X. & Puttonen, J. (2021). Factors affecting the performance of ventilation cavities in highly insulated assemblies. Journal of Building Physics 45(1), 67-110. https://doi.org/10.1177/1744259121995221

About the Authors

KLAUS VILJANEN

D. Sc. (Tech.)
Aalto University

Project Manager
Ramboll Finland Oy

Main research area
Building Physics, hygrothermal performance of the building external envelope

Address
Rakentajanaukio 4, 02150 Espoo, Finland
E-mail: klaus.viljanen@gmail.com

LAURINA FELIUS

Building Physics Consultant
Rambøll Norge AS, Trondheim, Norway

Main research area
Building physics, energy use in buildings, indoor climate

Address
Kobbes gate 2, 7042 Trondheim, Norway
E-mail: laurina.felius@ramboll.no